

# Very high frequency gravitational waves from magnetars and gamma-ray bursts

Hao Wen,<sup>\*</sup> Fangyu Li, Jin Li, and Zhenyun Fang

*Department of Physics, Chongqing University, Chongqing 401331, P.R. China*

(Dated: April 27, 2017)

## Abstract

Extremely powerful astrophysical electromagnetic (EM) system could be possible source of high-frequency gravitational waves (HFGWs). Here based on properties of magnetars and gamma-ray bursts (GRBs), we address “Gamma-HFGWs” (with very high frequency around  $10^{20} Hz$ ) caused by ultra-strong EM radiations (in the radiation-dominated phase of GRBs fireball) interacting with super-high magnetar surface magnetic fields ( $\sim 10^{11} Tesla$ ). By certain parameters of distance and power, the Gamma-HFGWs would have far field energy density  $\Omega_{gw}$  around  $10^{-6}$ , and they would cause perturbed signal EM waves of  $\sim 10^{-20} Watt/m^2$  in planned HFGW detection system based on EM response to GWs. Specially, Gamma-HFGWs would possess distinctive envelopes with characteristic shapes depending on particular structure of surface magnetic fields of magnetars, which could be exclusive features helpful to distinguish them from background noise. Results obtained suggest that magnetars could involve in possible astrophysical EM sources of GWs in very high frequency band, and Gamma-HFGWs would be potential targets for observations in the future.

**Keywords:** High-frequency gravitational waves, magnetar, gamma-ray bursts, gravitational wave source.

---

<sup>\*</sup> wenhao@cqu.edu.cn

## I. INTRODUCTION

LIGO had announced two direct detections of gravitational waves (GWs), in intermediate frequency band from source of black hole mergers[1, 2]. Such great events may inaugurate the era of GW astronomy, and it will also again arouse strong interest to look for GWs from various types of sources in different frequency bands (low, intermediate, high, and very high frequency bands). In this article we focus on a possible generation of very high frequency GWs (around  $10^{20}Hz$ ) from super-powerful astrophysical electromagnetic (EM) sources.

Actually, not only interaction between GWs and EM fields, but also generation of GWs from EM sources, had been long studied. E.g., B-mode polarization in cosmic microwave background (CMB) caused by very low-frequency primordial (relic) GWs[3–10], GWs generated by high-energy astrophysical plasma interacting with intense EM radiations[11], GWs produced by EM waves interacting with background magnetic fields[12–14], and EM response to HFGWs which would lead to perturbed signal EM waves [15–23]. For such issues, physical conditions and factors of the EM systems, like their strength, structure and scale, will crucially influence the energy and distribution of generated GWs and the displaying manner of perturbed signal EM waves (e.g., in proposed HFGW detectors).

Therefore, some celestial bodies having extraordinary EM environments, such as the magnetars (having ultrahigh surface magnetic fields), would act as natural astrophysical laboratories to provide extremely strong EM systems as possible GW sources. Thus, in some possible cases, e.g. a binary system consisting of magnetar and another celestial body which could emit super-powerful radiation of Gamma-ray bursts (GRBs), or, just only one magnetar but emitting GRBs itself, such systems would be strong EM sources of HFGWs by providing powerful EM waves to interact with ultra-high magnetic fields. In this paper, we address such “Gamma-HFGWs” and their possible characteristic properties.

Specifically, the Gamma-HFGWs would be produced by high-energy radiations of GRBs (up to  $10^{53}erg$  or even higher[24]) interacting with superstrong surface magnetic fields of magnetar ( $\sim 10^{11}Tesla$ )[25]. However, for conservative calculation, we only consider the contribution of such high-energy radiations within the radiation-dominated phase in the fireball of GRB where the radiation power decays quite fast by  $r^{-4}$  (because of the conversion of radiation photons into electron-positron pairs during the transition process into matter-

dominated phase[26]). Based on Einstein-Maxwell equations[12, 27] in frame of general relativity, such radiation and surface magnetic fields will provide a fast varying energy-momentum tensor  $T^{\mu\nu}$  as a powerful HFGW source. By typical parameters, we estimate that the Gamma-HFGWs (with very high frequency  $\sim 10^{20}Hz$ ) would have energy density  $\Omega_{gw}$  around  $10^{-6}$  at observational distance of  $\sim Mpc$  away from the source. This level of  $\Omega_{gw}$  could cause perturbed signal EM waves of strength  $\sim 10^{-20}Watt/m^2$  in the proposed HFGW detector based on EM response to HFGWs and synchro-resonance effect[14–20].

It should be noticed that, only components of magnetic fields which are perpendicular to propagating direction of radiation of GRBs, will contribute to the generation of Gamma-HFGWs[12, 27] (could be called as “perpendicular condition”). Thus the angular distributions of Gamma-HFGWs will appear in special patterns (e.g. dipole- or quadrupole-like patterns) accordant to specific mode and structure of the surface magnetic fields (their exact structure is still unknown so far, so we here employ a typical possible form[28] as an example for this paper). Due to misalignment of rotational axis and magnetic axis of magnetar, it would lead to particular pulse-like envelopes of energy density of Gamma-HFGWs in the observational direction. Such unique envelopes would be distinctive properties and criteria to distinguish the signals of Gamma-HFGWs from background noise.

The plan of this paper is as follows. In Sect.II, employed form of superstrong surface magnetic fields of magnetars are presented. In Sect.III, generation of Gamma-HFGWs and their energy density are estimated. In Sect.IV, characteristic envelopes of Gamma-HFGWs are expressed. In Sect.V, summary, conclusion and discussion are given.

## II. MODEL OF SUPERSTRONG SURFACE MAGNETIC FIELDS OF MAGNETAR

The structure of magnetic fields of magnetar, will essentially impact their interaction with EM waves. However, so far, we are not sure about the concrete form of surface distribution of such magnetic fields, although it’s well-known that magnetars can have extremely strong surface magnetic fields reaching to  $\sim 10^{11}Tesla$  or even higher[25]. Thus, in this paper, we take a typical form[28] of magnetic fields of magnetar as an example and basis for calculations

in the later sections, i.e., the surface magnetic fields could be generally expressed as[28]:

$$\mathbf{B}^{surf}(1, 0) = \vec{\nabla} \times (\vec{r} \times \vec{\nabla} S), \quad (1)$$

The scalar function  $S$  can be expanded in a series of spherical harmonics:

$$\begin{aligned} S &= S(l, m) = S_l^m(r) Y_l^m(\theta, \phi), \\ \text{and } Y_l^m(\theta, \phi) &= P_l^m(\cos \theta) e^{im\phi}; \end{aligned} \quad (2)$$

where  $P_l^m(\cos \theta)$  is Legendre polynomial. For  $l = 1, m = 0$  (corresponding to the dipole mode), it gives:

$$\begin{aligned} S(1, 0) &= C \frac{\cos \theta}{r^2} \sum_{\nu=0}^{\infty} a_{\nu} \left( \frac{2M}{r} \right)^{\nu}, \\ a_0 &= 1, a_{\nu} = \frac{(1 + \nu)^2 - 1}{(3 + \nu)\nu} a_{\nu-1}, (\text{for } \nu \geq 1), \end{aligned} \quad (3)$$

From Eqs.(1) to (3), it gives,

$$\begin{aligned} \mathbf{B}^{surf}(1, 0) &= \vec{\nabla} \times (\vec{r} \times \vec{\nabla} S(1, 0)) \\ &= C_1 \cos \theta \frac{1}{r^3} \sum_{\nu=0}^{\infty} a_{\nu} \left( \frac{2M}{r} \right)^{\nu} \vec{e}_r \\ &\quad + C_1 \sin \theta \frac{1}{r^3 h} \sum_{\nu=0}^{\infty} (\nu + 1) a_{\nu} \left( \frac{2M}{r} \right)^{\nu} \vec{e}_{\theta}, \end{aligned} \quad (4)$$

By calculations of the summation terms in Eq.(4), a typical analytical expression of the surface magnetic field of magnetar could be written as [see Fig.1(a)]:

$$\begin{aligned} \mathbf{B}_{di}^{surf}(1, 0) &= 2C_1 \cos \theta \frac{1}{r^3} \frac{-3r[r^2 \log(1 - \frac{2M}{r}) + 2M(M + r)]}{8M^3} \vec{e}_r \\ &\quad + C_1 \frac{\sin \theta}{r^3 h} \frac{3r^2[2M(\frac{M}{r-2M} + 1) + r \log(1 - \frac{2M}{r})]}{4M^3} \vec{e}_{\theta}, \end{aligned} \quad (5)$$

the metric  $h$  is defined as[28]:

$$h = h(r) = \left(1 - \frac{2M}{r}\right)^{-\frac{1}{2}}, M = \frac{Gm(r)}{c^2}, \quad (6)$$

$m(r)$  is the mass function that determines the total mass enclosed within the sphere of radius  $r$ , and  $m(r) \equiv$  magnetar mass in our case because we only concern magnetic fields outside magnetars. Here,  $C_1$  and  $C_2$  (see below) are constants that have been calibrated to typical strengths of surface magnetic fields (e.g.  $10^{11}T$ ).

Similarly, for the case of  $l = 2, m = 0$ , we have the quadrupole form of surface magnetic fields [Fig.1(b)]:

$$\begin{aligned} \mathbf{B}_{quad}^{surf}(2, 0) = & 3C_2(3 \cos^2 \theta - 1) \frac{1}{r^4} \\ & \cdot \frac{-3r[r^2 \log(1 - \frac{2M}{r}) + 2M(M + r)]}{8M^3} \vec{e}_r \\ & + 3C_2 \cos \theta \sin \theta \frac{1}{r^4 h} \\ & \cdot \frac{3r[2M(\frac{4M^2}{r-2M} + M + r) + r^2 \log(1 - \frac{2M}{r})]}{8M^3} \vec{e}_\theta, \end{aligned} \quad (7)$$

For magnetars, the surface magnetic fields in quadrupole mode would have comparable

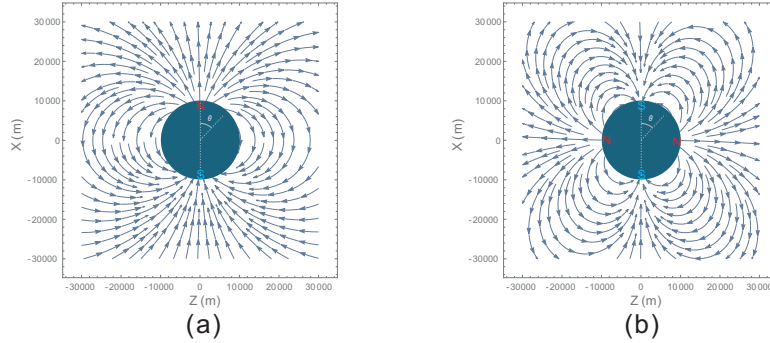


**FIG. 1. Two-dimensional presentations of models of magnetar surface magnetic fields in dipole and quadrupole modes.** Poloidal components of dipole mode (a) and quadrupole mode (b) surface magnetic fields of magnetar reach their maximum at polar angle  $\theta = \pi/2$  and  $\theta = \pi/4, 3\pi/4$  respectively. Patterns of surface magnetic fields will crucially influence the angular distributions of Gamma-HFGWs.

strength to that of dipole mode[29]. In dipole mode, the poloidal components [see  $\vec{e}_\theta$  component in Eq.(5)] have the maximal values at polar angle  $\theta = \pi/2$  [Fig.1(a)], and the radial components [see  $\vec{e}_r$  component in Eq.(5)] have their maximum around polar angle  $\theta = 0$  and  $\pi$  (two magnetic poles). Differently, in quadrupole mode the poloidal components [see  $\vec{e}_\theta$  component in Eq.(7)] have maximal values around  $\theta = \pi/4$  and  $3\pi/4$  [Fig.1(b)]. These particular distributions of surface magnetic fields will act key roles to determine the angular distributions of the Gamma-HFGWs generated by EM sources from magnetars (see

following sections).

### III. GAMMA-HFGWS FROM MAGNETARS AND GRBS

Extremely powerful radiations (around  $\sim 10^{51}$  to  $10^{53} \text{erg}$  or even higher in a few seconds) make GRBs the most luminous (electromagnetically) objects in the Universe[26, 30, 31]. According to general relativity, interactions between such radiation of high energy EM bursts and ultra-intense surface magnetic fields of magnetars( $\sim 10^{11}T$  or higher[25]), can provide a fast varying energy momentum tensor  $T^{\mu\nu}$  as a strong EM source of HFGWs in very high frequency band (denoted as “Gamma-HFGWs”, the same hereafter).

Lots of models of inner engine of GRBs had been proposed to explain the origin of so huge amount of energy, such as black-hole accretion, collapsar model, supernova model (see review by Piran[24]), binary neutron star mergers[32, 33], black hole-neutron star mergers[34], Blandford-Znajek mechanism[35], pulsar model[24, 36–41], magnetar model[42–45], etc. Specially, the magnetar model of GRBs with fireball scenarios are studied by some previous works[46–51], and a possible case is to consider fireball trapped near the magnetar surface by the superstrong magnetic fields[52–58]. Therefore, no matter in the case that GRBs source would combine magnetar as a binary system, or in the case that magnetar itself would become the source of GRBs, once such GRB radiations interact with the magnetar surface magnetic fields, it could lead to considerable generation of Gamma-HFGWs.

GRBs have complicated process and mechanism, especially for the problem of inner engine that produces the relativistic energy flow[26]. According to fireball internal-external shocks model, the generation of observed GRBs would be on account of the process of kinetic energy of ultrarelativistic flow to dissipate during the internal collisions (internal shocks)[24]. Piran had summed[26] generic pictures to suggest that in the fireball model the GRBs are composed of several stages: (i) a compact inner “engine” to produce a relativistic energy flow, (ii) stage of energy transportation, (iii) conversion of this energy to observed prompt radiation, (iv) conversion of the remaining energy to afterglow.

For stage(i), Goodman[59] and Paczynski[60] who proposed the relativistic fireball model had shown that the sudden release of a large quantity of gamma-ray photons into such compact region can lead to an opaque photon-lepton fireball (pairs-radiation plasma, by

production of electron-positron pairs from photon-photon scattering)[26], because if the photon energy reaches high enough ( $> 511\text{KeV}$ ), electron-positron pairs can be formed from the radiations.

Thereafter, pairs-radiation plasma behaves like a perfect fluid and expands by its own pressure[26]. During this expansion and energy transportation stage, the expanding fireball has two basic phases[26]: a radiation-dominated phase and a matter-dominated phase (see Fig.2). In early stage of radiation-dominated phase, most energy comes out as high-energy radiation[61], and the fluid of plasma accelerates in the process of expansion with very large Lorentz factors, and then a transition from the radiation-dominated phase to the matter-dominated phase takes place when the fireball has a size about  $10^7 m$  (typical value)[26]. Crucially, in the radiation-dominated stage, energy of radiation decays by  $distance^{-4}$  (much faster than normal spherical radiation in free space which decays by  $distance^{-2}$ , due to the formation of electron-positron pairs from photons, see details in sec.6.3 of ref.[26]).

Therefore, although GRBs have complex process, in early stage of the radiation-dominate phase, the photon energy still dominate in the fireball and it can interact with extremely strong magnetar surface magnetic fields to become a considerable EM source of Gamma-HFGWs (Fig.2). While, for conservative estimation, here we will consider only much shorter interaction range for calculation (of generation of Gamma-HFGWs) in the very early stage of radiation-dominate phase, i.e., only consider the interaction range from  $10^4 m$  (supposed magnetar radius) to  $2 \times 10^4 m$ .

In local area, for a specific propagation direction (i.e. z-direction), the energy flux density of this strong EM source of Gamma-HFGWs can be represented by “0-3” component of energy momentum tensor  $T^{03(1)}$ [17]:

$$\begin{aligned} T^{03(1)} &= \frac{-1}{\mu_0} (F_{\alpha}^{0(0)} \tilde{F}^{3\alpha(1)} + \tilde{F}_{\alpha}^{0(1)} F^{3\alpha(0)}) \\ &= \frac{-1}{\mu_0} [0 + \tilde{F}_1^{0(1)} F^{31(0)}] = \frac{1}{\mu_0 c} \tilde{E}_x^{(1)burst} e^{i(kz-\omega t)} B_{\theta}^{(0)surf}, \end{aligned} \quad (8)$$

Here, “ $k$ ” and  $\tilde{F}^{\mu\nu(1)}$  are wave vector and EM tensor of EM waves of GRBs;  $F^{\mu\nu(0)}$  is EM tensor of surface magnetic fields. Here we define the outward radial direction as z-direction, i.e.,  $F^{31(0)} = -F^{13(0)} = -B_y^{(0)surf} = B_{\theta}^{(0)surf} = 10^{11} T$  (simply treat other components as

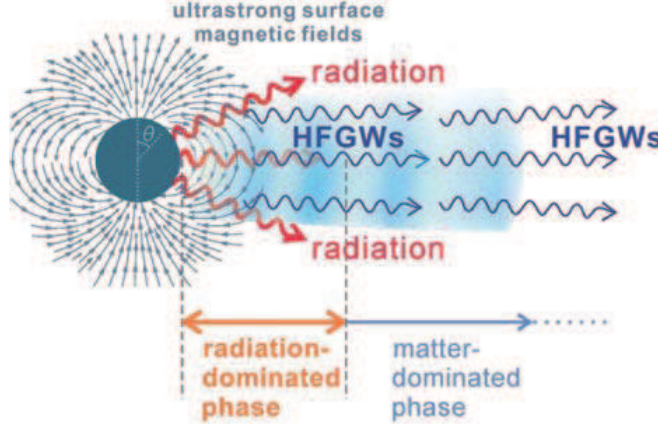


FIG. 2. **Gamma-HFGWs caused by strong radiations (in radiation-dominated phase of fireball in GRBs) interacting with ultrastrong surface magnetic fields (dipole mode) of magnetar.** Expanding fireball has two basic phases: radiation-dominated phase (typically  $< 10^7 m$ ) and matter-dominated phase ( $> 10^7 m$ )[26]. In radiation-dominated stage, energy of strong radiation decays quite quickly by  $distance^{-4}$ [26]. However, in very early stage of the radiation-dominated phase, photon energy still dominates in the fireball and can provide extremely powerful EM source to interact with the strong surface magnetic fields, i.e. provide a fast varying energy momentum tensor  $T^{\mu\nu}$  as a strong EM source of generation of Gamma-HFGWs, and such HFGWs are transparent to the optically-thick fireball. This figure is an intuitive demonstration and the scale is not exact.

zero, because only the  $B_{\theta}^{(0)surf}$  [poloidal component of the surface magnetic fields, e.g.  $\vec{e}_{\theta}$  components in Eqs.(5) and (7)] which is perpendicular to the direction of GRBs in supposed configuration here, will contribute to the generation of HFGWs[12, 27] (noted as “perpendicular condition”, the same hereafter). Thus, through magnetar surface magnetic fields in dipole-mode, generated HFGWs will also follow a dipole-like pattern, i.e., their angular distribution mainly concentrate around the region of polar angle  $\theta = \pi/2$  (equator area). Differently, through magnetar surface magnetic fields in quadrupole-mode, generated Gamma-HFGWs would radiate in a quadrupole pattern concentrating around  $\theta = \pi/4$  and  $3\pi/4$ .

For estimating such Gamma-HFGWs, we can first focus on a very thin layer in local area, where the radiation and surface magnetic fields can be treated uniform, so the generation



of Gamma-HFGWs can be expected by the linearized Einstein field equation:

$$\begin{aligned}\square \tilde{h}^{\mu\nu}(z, t) &= -\frac{16\pi G}{c^4} T^{\mu\nu} \\ &= -\frac{16\pi G}{c^4} \cdot \frac{1}{\mu_0 c} \tilde{E}_x^{(1)burst} e^{i(kz - \omega_\gamma t)} B_\theta^{(0)surf}\end{aligned}\quad (9)$$

A solution of above equation can be obtained:

$$\begin{aligned}\tilde{h}^{\mu\nu}(z, t) &= A^\gamma e^{i(kz - \omega t + \frac{3\pi}{2})} \\ &= \frac{-z 8\pi G \tilde{E}_x^{(1)burst} B_\theta^{(0)surf}}{k c^5 \mu_0} e^{i(kz - \omega_\gamma t + \frac{3\pi}{2})},\end{aligned}\quad (10)$$

this local solution of planar GWs caused by uniform EM source clearly shows that the accumulation effect (because the HFGWs caused by radiation will be accumulated during their propagation along with the radiation synchronously due to their identical speed of light) is proportion to the accumulative distance (term “ $z$ ”), which is totally accordant to previous results of accumulation effect for case of planar GWs[13].

However, for our case of the Gamma-HFGWs, the situation is much more complicate, i.e., the background magnetic fields (surface magnetic fields of the magnetar) will nonlinearly decrease along the radial direction [Eqs.(5) and (7)], and the radiation will also decay in the ratio of  $\sim 1/z^4$  in the radiation-dominated phase (within distance  $< 10^7 m$ )[26]. Thus the compositive contribution of process of generation of Gamma-HFGWs is very different to scenario of GW generation[12] from interaction of planar EM waves with uniform magnetic fields. E.g., for a certain power produced by GRB inner engine (noted as  $P_{total}^\gamma$ ), energy flux density of the EM waves at distance of  $r_0$  (radius of magnetar) should be  $P_{total}^\gamma / 4\pi r_0^2 \sim (\tilde{E}_{x.r_0}^{(1)burst})^2 / (\mu_0 c)$ . Thus, at distance of  $z$ , electric component of the radiation is  $\tilde{E}_x^{(1)burst} = \tilde{E}_{x.r_0}^{(1)burst} \cdot r_0^2 / z^2$ .

Therefore, to obtain expression of accumulated amplitude of the Gamma-HFGWs ( $A_{accum}^\gamma$ ), we can integrate Gamma-HFGWs generated within very thin local layers [with accumulative distance of  $dr$ , where we can employ Eq.(10)] from the magnetar surface to a certain larger distance  $r$ . If taking dipole surface magnetic field [ $B_\theta^{(0)surf}$ , from the second

part of Eq.(5)], it can be worked out:

$$\begin{aligned}
A_{accum}^{\gamma}(z) &= \int_{r_0}^z \frac{8\pi G}{kc^5\mu_0} (\tilde{E}_{x.r_0}^{(1)burst} \cdot \frac{r_0^2}{r^2}) B_{\theta}^{(0)surf} \cdot \frac{r}{z} dr \\
&= \frac{3C_1 r_0^2 \tilde{E}_{x.r_0}^{(1)burst} \frac{8\pi G}{kc^5\mu_0}}{4hM^3 z} \sin \theta \\
&\cdot \int_{r_0}^z \frac{r^2 [2M (\frac{M}{r-2M} + 1) + r \ln (1 - \frac{2M}{r})]}{r^4} dr \\
&= \frac{3C_1 r_0^2}{z 8M^3 h} \cdot \frac{8\pi G}{kc^5\mu_0} \tilde{E}_{x.r_0}^{(1)burst} \sin \theta \\
&\cdot [-\frac{2M}{z} + \ln(1 - \frac{2M}{z}) + 2\text{Li}_2 \frac{2M}{z} \\
&+ \ln \frac{r_0}{r_0 - 2M} - 2\text{Li}_2 \frac{2M}{r_0} + \frac{2M}{r_0}];
\end{aligned} \tag{11}$$

here,  $Li_2(\frac{2M}{r_0}) = \sum_{k=1}^{\infty} \frac{(2M/r_0)^k}{k^2}$  is polylogarithm function of order 2 with argument  $\frac{2M}{r_0}$ , similarly hereafter. Eq.(11) looks complicated, but actually if we take only the first order of  $Li_2(\frac{2M}{z})$  (i.e.,  $\frac{2M}{z}$ ), the Eq.(11) has simple asymptotic behavior in large distance:

$$A_{accum}^{\gamma}(z) \rightarrow p1 \cdot z^{-1} + p2 \cdot z^{-2} \tag{12}$$

where

$$\begin{aligned}
p1 &= \frac{3C_1 r_0^2}{M^3 h} \cdot \frac{\pi G}{kc^5\mu_0} \tilde{E}_{x.r_0}^{(1)burst} \sin \theta \\
&\cdot (\ln \frac{r_0}{r_0 - 2M} - 2\text{Li}_2 \frac{2M}{r_0} + \frac{2M}{r_0}). \\
p2 &= \frac{3C_1 r_0^2}{4M^2 h} \cdot \frac{8\pi G}{kc^5\mu_0} \tilde{E}_{x.r_0}^{(1)burst} \sin \theta;
\end{aligned} \tag{13}$$

Similarly, for surface magnetic fields in quadrupole mode  $[B_{\theta-quad}^{(0)surf}]$ , from the second part

of Eq.(7)], accumulated amplitude of Gamma-HFGWs can be given:

$$\begin{aligned}
A_{accum}^{\gamma-quad}(z) &= \int_{r_0}^z \frac{8\pi G}{kc^5\mu_0} (\tilde{E}_{x.r_0}^{(1)burst} \cdot \frac{r_0^2}{r^2}) B_{\theta-quad}^{(0)surf} \cdot \frac{r}{z} dr \\
&= \frac{9\pi G C_2 \sin \theta \cos \theta \tilde{E}_{x.r_0}^{(1)burst} r_0^2}{kc^5\mu_0 h M^3 z} \left\{ \frac{-2}{r_0} + \frac{2M^2}{3} \left( \frac{-1}{r_0^3} + \frac{1}{z^3} \right) \right. \\
&\quad + \frac{2}{z} + \frac{\ln(1 - 2M/r_0)}{r_0} - \frac{\ln(1 - 2M/z)}{z} \\
&\quad \left. + \left[ \ln \frac{r_0}{r_0 - 2M} + \ln \left( 1 - \frac{2M}{z} \right) \right] / M \right\}. \tag{14}
\end{aligned}$$

TABLE I. For some parameters in possible range (not limit to that have already been confirmed by current observations), we estimate accumulated energy density ( $\Omega_{gw}$ , at far observational distance) of the Gamma-HFGWs generated by interaction between powerful radiation of GRBs and ultra-high surface magnetic fields of magnetars. Representative frequency of Gamma-ray (also of the Gamma-HFGWs) is set to  $\sim 10^{20} Hz$ . Shaded cells in the table indicate the parameter range where the Gamma-HFGWs would cause perturbed signal EM waves of  $\sim 10^{-20} W/m^2$  in proposed HFGW detector[14–18] meanwhile corresponding power of GRBs would decay into about  $30 Watt/m^2$  (which is safe, since it is far less than the power able to cause globally ozone depletion and to result in extinction of lives[62]). Therefore, the shaded cells represent the Gamma-HFGW sources with optimal parameters to be possible potential observational targets in the future.

Observational distance away from magnetar	Dipole mode, $B^{surf} = 4 \times 10^{11} T$ , $P_{total}^{\gamma} (erg \cdot s^{-1})$		
	$3 \times 10^{54}$	$3 \times 10^{52}$	$3 \times 10^{50}$
$\sim 10 kpc$	$\Omega_{gw}^{\gamma} : 1.2 \times 10^{-2}$	$1.2 \times 10^{-4}$	$1.2 \times 10^{-6}$
$\sim 100 kpc$	$\Omega_{gw}^{\gamma} : 1.2 \times 10^{-4}$	$1.2 \times 10^{-6}$	$1.2 \times 10^{-8}$
$\sim Mpc$	$\Omega_{gw}^{\gamma} : 1.2 \times 10^{-6}$	$1.2 \times 10^{-8}$	$1.2 \times 10^{-10}$
$\sim 10 Mpc$	$\Omega_{gw}^{\gamma} : 1.2 \times 10^{-8}$	$1.2 \times 10^{-10}$	$1.2 \times 10^{-12}$
$\sim Gpc$	$\Omega_{gw}^{\gamma} : 1.2 \times 10^{-12}$	$1.2 \times 10^{-14}$	$1.2 \times 10^{-16}$

So far, lots of confirmed magnetars are in the Milky way and can have short distance  $\sim kpc$ , but all currently observed GRBs are from distant galaxies outside the Milky way, and the nearest one is GRB 980425 with redshift  $z = 0.0085$  or about 36 Mpc away. Even if any GRB happens in distance of  $\sim kpc$ , it would cause globally ozone depletion and may lead to great ecological damage and extinction of the life on the Earth (this had been believed

as a possible reason of the late Ordovician mass extinction[62]). Therefore, as presented in Table I, if some magnetars in proper distance with GRBs of suitable power, they still could provide far field effect of Gamma-HFGWs on the Earth (or far field observation points) and meanwhile the power of Gamma-ray can decay into a safe level.

E.g., if the maximum of surface magnetic fields of magnetar  $\sim 10^{11} Tesla$ ,  $P_{total}^{\gamma} \sim 10^{54} erg \cdot s^{-1}$ , magnetar distance  $\sim 1 Mpc$ , then the energy density  $\Omega_{gw}$  of Gamma-HFGW at the Earth could be  $\sim 10^{-6}$  [here,  $\Omega_{gw} = \frac{\pi^2}{3} h^2 (\nu/\nu_H)^2$ , where  $\nu_H$  is present Hubble frequency,  $h$  is GW amplitude]. Meanwhile, in this case, power of GRB around the globe is only about  $30 Watt \cdot m^{-2}$  which is in a safe level far less than the order of magnitude to cause global ozone depletion[62]. Other possible cases with suitable parameters of distance and GRB power are also shown in the shaded cells in Table I. We can find that,  $\Omega_{gw}$  in cells with larger distance than these shaded cells, will have too low energy density for potential detection (e.g. in proposed HFGW detectors[14–18]), and cells with shorter distance than these shaded cells can have higher  $\Omega_{gw}$  but will lead to stronger GRB power which would be dangerous to the life and ecological system on the Earth. Therefore, the shaded cells in Table I present optimal range of Gamma-HFGW sources with proper distance and suitable power (in safe level near globe) to be potentially observational targets of HFGWs from the Earth. Nevertheless, for other cases which can not provide sizable far field effect on the Earth, such as more faraway GRBs, the possibility still would not be excluded that in the future some spacecraft-based HFGW detector approaching closer area to such sources or some Earth-based detector with greatly enhanced sensitivity would also might be able to capture these Gamma-HFGWs.

Some proposed HFGW detection system[14–18] is specially sensitive to GWs in very high frequency bands. E.g., the Gamma-HFGWs ( $\Omega_{gw} \sim 10^{-6}$ ) would generate the first-order perturbed signal EM waves having power of  $\sim 10^{-20} Watt$  per  $m^2$  in such planned detection system. However, issues about how to experimentally extract and distinguish such perturbed EM signals and relevant techniques, are not key points in this paper, and related topics will be addressed in other works.

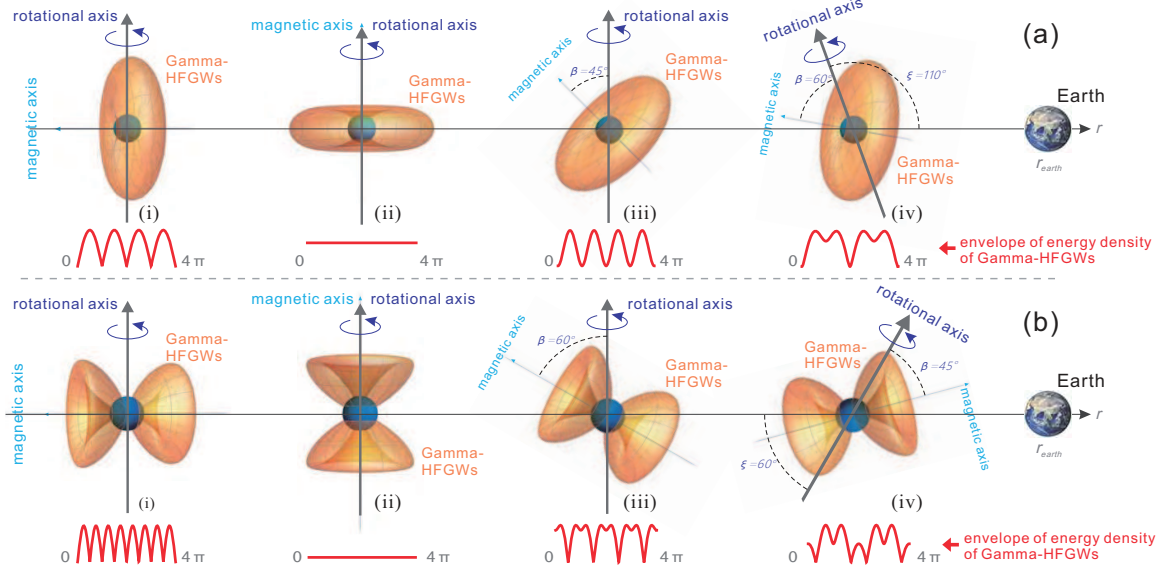


FIG. 3. **Diverse angular configurations would cause characteristic envelopes of Gamma-HFGWs.** This plot intuitively explains how various distinctive Gamma-HFGW envelopes received at the Earth (or at far field observation point) can be formed according to different angular sets (angle  $\beta$  between rotational and magnetic axis, and angle  $\xi$  between rotational axis and observational direction). Energy of Gamma-HFGWs facing to the Earth will fluctuate with respect to the rotational phase, and then lead to diverse envelopes of the energy density of Gamma-HFGWs, similar to the formation of pulsing signals from the pulsars. Sub-figure(a) and (b) show examples of distinctive envelopes by different  $\beta$  and  $\xi$ , of dipole-pattern and quadrupole-pattern Gamma-HFGWs (see Eqs.15 and 16). Here  $\xi$  is  $90^\circ$  in cases (i)-(iii), and  $\beta$  is  $90^\circ$ ,  $0^\circ$ ,  $45^\circ$  and  $60^\circ$  for cases (i) to (iv), respectively. For some angular sets, envelopes could be more complicated, e.g. in case (iv) they appear in unusual distinctive shapes containing both higher and lower mixed peaks.

#### IV. CHARACTERISTIC ENVELOPE OF GAMMA-HFGWS

Special geometrical information of structure of magnetar surface magnetic fields, could lead to characteristic envelope of energy density of Gamma-HFGWs at observation direction, and such special feature of these GW signals can be very helpful to distinguish them among background noise.

However, the exact structure of magnetar surface magnetic fields still is unclear so far. Nevertheless, here, as mentioned above, we can take the form of magnetar magnetic fields[28] as an example, to present how particular surface magnetic fields lead to corresponding special GW envelopes. In detail, due to that the rotational axis and magnetic axis of magnetar are usually not identical, so during one period, the maximums of Gamma-HFGWs will not

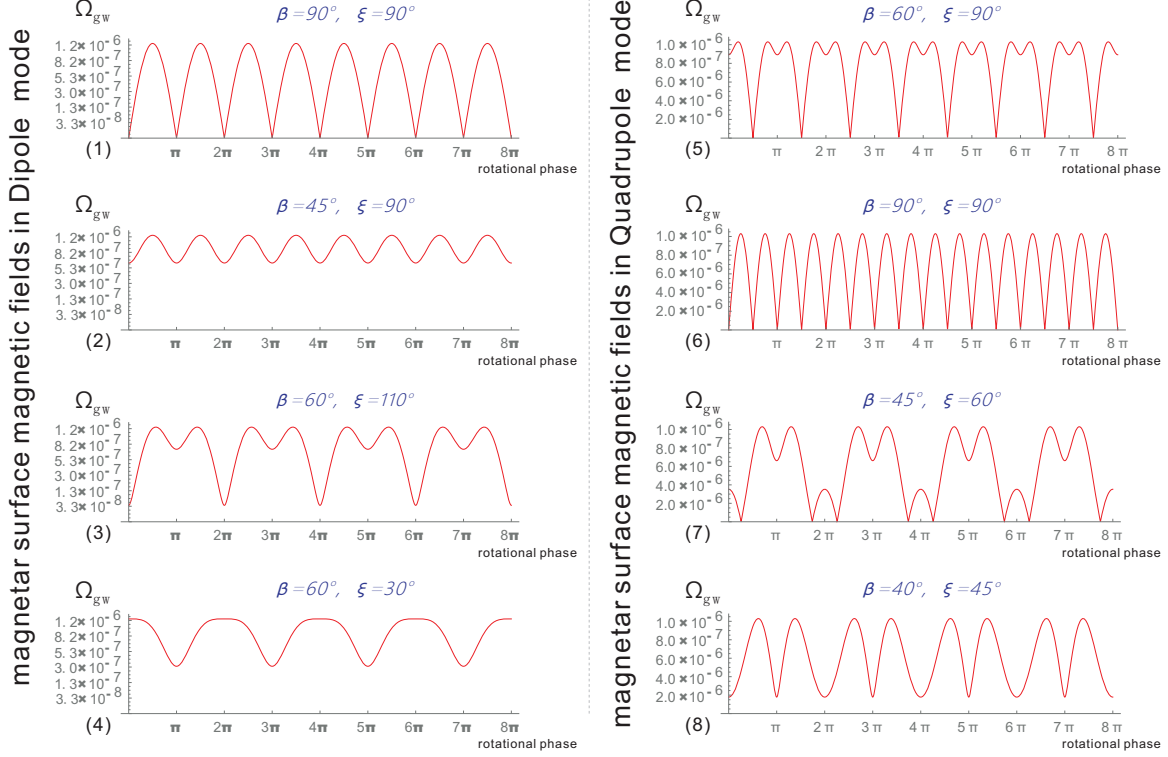


FIG. 4. **Examples of energy density envelopes of Gamma-HFGWs at the Earth or far field observation points.** Typical envelopes of energy density of Gamma-HFGW are estimated for both dipole case[sub-figure(1) to (4), see Eq.15] and quadrupole case[sub-figure(5) to (8), see Eq.16] in various angles  $\beta$  and  $\xi$  (as the same defined as those in the Fig.3). Parameters for dipole case are: observation distance =  $1\text{Mpc}$ ,  $P_{total}^\gamma = 3 \times 10^{54} \text{ erg/s}$ ,  $B_{surf} = 4 \times 10^{11} \text{ T}$ , and parameters for quadrupole case are:  $P_{total}^\gamma = 6 \times 10^{54} \text{ erg/s}$ ,  $B_{surf} = 5 \times 10^{11} \text{ T}$ . These particular envelopes would be helpful to distinguish the Gamma-HFGWs out of background noise in possible detection schemes.

always directly point to the observation direction. Therefore, envelopes of energy density of these Gamma-HFGWs will vary and fluctuate periodically according to the rotation of magnetar. It is similar to the mechanism of pulsing signals from pulsars (where the misalignment between these two axis of pulsars usually causes the peak of EM radiations facing to the Earth once for every spin period).

In Fig.3, we present that in different values of angles (i.e. angle between magnetic and rotational axis, noted as  $\beta$ , and angle between rotational axis and observation direction, noted as  $\xi$ ), envelopes of energy density of Gamma-HFGWs would particularly appear in some pulse-like patterns with various distinctive shapes. By using  $\Omega_{gw} = \frac{\pi^2}{3} h^2 (\nu/\nu_H)^2$  and Eqs.(11) to (14), with coordinate transformation, we can have analytical expressions of envelopes of energy density of Gamma-HFGWs at the Earth or far field observation points

(here  $\Omega_{gw}^{\gamma-di}$  and  $\Omega_{gw}^{\gamma-quad}$  are for dipole and qudrupole cases respectively):

$$\Omega_{gw}^{\gamma-di} = \frac{\pi^2}{3} (A_{accum}^{\gamma}|_{\theta=\pi/2})^2 \left(\frac{\nu}{\nu_H}\right)^2 \cdot [(\sin \xi \cos \beta \cos \varphi + \cos \xi \sin \beta)^2 + \sin^2 \xi \sin^2 \varphi], \quad (15)$$

and for the quadrupole case,

$$\Omega_{gw}^{\gamma-quad} = \frac{\pi^2}{3} (A_{accum}^{\gamma-quad}|_{\theta=\pi/4})^2 \left(\frac{\nu}{\nu_H}\right)^2 \cdot (\cos \xi \cos \beta - \sin \xi \sin \beta \cos \varphi)^2 \cdot [(\sin \xi \cos \beta \cos \varphi + \cos \xi \sin \beta)^2 + \sin^2 \xi \sin^2 \varphi]. \quad (16)$$

TABLE II. Given different effective accumulation distance  $D$  of Gamma-HFGWs sources, decay parameter  $\Lambda$  of effective radiation in GRBs, decay parameter  $\Xi$  of effective strong background magnetic fields, estimated energy density of effective-Gamma-HFGWs ( $\Omega_{gw}^{\gamma-eff}$ ) in far field regions are given. Here  $P_{total}^{\gamma}$  is assumed  $5 \times 10^{54} \text{ erg/s}$ , and far field observational distance sets to  $3.3 \text{ Mpc}$  from the magnetar.

effective accumulation distance around source	far field (3.3Mpc) $\Omega_{gw}^{\gamma-eff}$ by different decaying parameters $\Lambda$ and $\Xi$
	$\Lambda = 2, \Xi = 1; \Lambda = 2, \Xi = 2; \Lambda = 2, \Xi = 3; \Lambda = 2, \Xi = 4; \Lambda = 4, \Xi = 5$
$D = 10 \text{ km}$	$\Omega_{gw}^{\gamma-eff} :$ $5.3 \times 10^{-6} \quad 3.0 \times 10^{-6} \quad 1.8 \times 10^{-6} \quad 1.1 \times 10^{-6} \quad 4.3 \times 10^{-7}$
$D = 100 \text{ km}$	$\Omega_{gw}^{\gamma-eff} :$ $1.7 \times 10^{-5} \quad 5.2 \times 10^{-6} \quad 2.3 \times 10^{-6} \quad 1.3 \times 10^{-6} \quad 4.3 \times 10^{-7}$

For different values of  $\beta$  and  $\xi$ ,  $\Omega_{gw}$  of Gamma-HFGWs have various distinctive envelopes with respect to rotational phase  $\varphi$  (Fig.3), but unlike the pulsars, above envelopes will usually (but not always) come with two peaks during every rotational period [for dipole-mode surface magnetic fields, see Fig.3(a), i.e. the frequency of pulses is double to the rotational frequency], or usually with four peaks for every rotational period [for case with quadrupole-mode surface magnetic fields, see Fig.3(b)], due to special angular distributions of Gamma-HFGWs (see Fig.3). Based on Eqs.(15) and (16), typical curves of  $\Omega_{gw}$  envelopes of Gamma-HFGWs can be estimated [see Fig.4(1)-(4) for dipole case and (5)-(8) for quadrupole case]. The characteristic envelopes would be helpful to distinguish the Gamma-HFGWs out of background noise, no matter for the model of magnetar magnetic fields we take here, or for other models with different structures.

Mechanism of GRBs is actually quite complex, more detailed issues of generation of HFGWs based on fireball model or other models such as poynting flux model[24, 36–40], involving magnetars or black holes or even other sources, can be further studied as consequent works. However, approximated estimations can be addressed here for some possible situations. E.g., in various magnetar and GRB models, we always can assume that effective (for HFGW generation) EM radiations decay by  $r^\Lambda$  ( $r$  is distance), and assume strong magnetic fields (contributing to HFGW generation) decay in  $r^\Xi$ . For typical  $r^\Lambda$ ,  $r^\Xi$  and effective accumulation distance  $D$  (for interaction between EM radiations and strong magnetic fields), accumulated “effective-Gamma-HFGWs” generally have the form (for cases of  $\Lambda + \Xi \neq 2$ ):

$$\begin{aligned}
A_{accum}^{\gamma-eff}(z) &= \int_{r_0}^D \frac{8\pi G}{kc^5\mu_0} \tilde{E}_{x.r_0}^{(1)burst} \left(\frac{r_0}{r}\right)^\Lambda \\
&\cdot B_{\theta-Max}^{(0)surf} \left(\frac{r_0}{r}\right)^\Xi \cdot \frac{r}{z} dr \\
&= \frac{8\pi G \tilde{E}_{x.r_0}^{(1)burst} B_{\theta-Max}^{(0)surf}}{kc^5\mu_0} \frac{1}{D} \frac{r_0^2 - D^2 \left(\frac{r_0}{D}\right)^{\Lambda+\Xi}}{\Lambda + \Xi - 2};
\end{aligned} \tag{17}$$

or for cases of  $\Lambda + \Xi = 2$ , it is:

$$A_{accum}^{\gamma-eff}(z) = \frac{8\pi G \tilde{E}_{x.r_0}^{(1)burst} B_{\theta-Max}^{(0)surf}}{kc^5\mu_0} \frac{r_0^{\Lambda+\Xi}}{D} \ln \frac{D}{r_0}; \tag{18}$$

Table II gives estimations of energy density of above effective-Gamma-HFGWs at far field observation point, with short accumulation distance  $D$  around the source of magnetar, given different effective parameters  $r^\Lambda$  and  $r^\Xi$ . Here, we ignore sources of Gamma-HFGWs outside the accumulation distance  $D$ . We find some of these energy density (around  $10^{-6}$ ) would also suitable for the proposed HFGW detector[14–18].

## V. SUMMARY AND DISCUSSION

As powerful astrophysical bodies, magnetars could provide extremely strong celestial EM sources of HFGWs. This article attempts to address novel issues of generation of HFGWs (with very high frequency  $\sim 10^{20} Hz$ ) caused by interaction between ultra-high magnetar surface magnetic fields and strong radiations of GRBs. We summarize the main results as follows:



(1) We estimate the energy density  $\Omega_{gw}$  of Gamma-HFGWs. It's found that by certain parameters of observational distance and GRB power, the Gamma-HFGWs would have far field  $\Omega_{gw}$  around  $10^{-6}$  (Table I). Gamma-HFGWs having such energy density could cause the first-order perturbed signal EM waves of  $\sim 10^{-20} W/m^2$  in the proposed HFGW detection system based on EM response to HFGWs and synchro-resonance effect [14–20]. However, issues about how to extract and distinguish such perturbed EM signals and relevant concrete experimental techniques, are not key points in this paper, and they can be addressed in subsequent works. At least, with far field effect, Gamma-HFGWs would provide possible potential targets of HFGWs for observation in the future from the Earth or from far field observation points.

(2) More general and approximated estimations of generation of HFGWs by GRB radiations interacting with strong surface magnetic fields of magnetar, has also been addressed. Brief estimations show that even if such general EM sources decay very fast (Table II), they would still possibly lead to  $\Omega_{gw} \sim 10^{-5}$  to  $10^{-7}$  of HFGWs in observational distance of  $\sim 3.3 Mpc$ , given typical effective accumulation distance and various decaying ratio of the radiation and magnetic fields, and such levels would also be suitable for the proposed HFGW detector [14–20].

(3) We find the envelopes of energy density of Gamma-HFGWs strongly depend on the structure of surface magnetic fields of magnetars. E.g., for the model of magnetic fields of magnetar we employ here (in dipole or quadrupole modes), the envelopes would appear in distinctive pulse-like patterns [see Figs. 3, 4, based on estimated expressions of Eqs. (15), (16)]. In other words, such characteristic envelopes not only could deliver and reflect specific geometrical information of surface magnetic fields of magnetars, but also, they could be an exclusive identification criterion to distinguish Gamma-HFGWs from background noise.

In general, magnetars could involve in possible astrophysical EM sources of GWs in very high frequency bands, and the Gamma-HFGWs they produce would provide far field effects with distinctive characters, so they would be possible potential targets for observations in the future. If any Gamma-HFGWs can be detected, it may provide evidences not only

for HFGWs from superpowerful astrophysical process and celestial bodies, but also provide references for models of magnetars (including their inner structures and configuration of surface magnetic fields) and models of GRBs.

## ACKNOWLEDGMENTS

This work is supported by the National Natural Science Foundation of China (No.11605015, No.11375279, No.11205254, No.11647307), and the Fundamental Research Funds for the Central Universities (No.106112016CDJXY300002 and 106112015CDJRC131216).

- 
- [1] B. P. Abbott *et al.* (LIGO Scientific Collaboration and Virgo Collaboration), Phys. Rev. Lett. **116**, 061102 (2016).
  - [2] B. P. Abbott *et al.* (LIGO Scientific Collaboration and Virgo Collaboration), Phys. Rev. Lett. **116**, 241103 (2016).
  - [3] Y. Zhang, W. Zhao, Y. Yuan, and T. Xia, CHINESE PHYSICS LETTERS **22**, 1817 (2005).
  - [4] W. Zhao and M. Li, PHYSICS LETTERS B **737**, 329 (2014).
  - [5] W. Zhao and Y. Zhang, Phys. Rev. D **74**, 083006 (2006).
  - [6] P. A. R. Ade, Y. Akiba, A. E. Anthony, K. Arnold, M. Atlas, *et al.*, Phys. Rev. Lett. **113**, 021301 (2014).
  - [7] D. Baskaran, L. P. Grishchuk, and A. G. Polnarev, Phys. Rev. D **74**, 083008 (2006).
  - [8] B. G. K. A. G. Polnarev, N. J. Miller, Monthly Notices of the Royal Astronomical Society **386**, 1053 (2008).
  - [9] U. Seljak and M. Zaldarriaga, Phys. Rev. Lett. **78**, 2054 (1997).
  - [10] J. R. Pritchard and M. Kamionkowski, Ann. Phys. (N.Y.) **318**, 2 (2005).
  - [11] M. Servin and G. Brodin, Phys. Rev. D **68**, 044017 (2003).
  - [12] M. E. Gertsenshtein, Sov. Phys. JETP **14**, 84 (1962).
  - [13] D. Boccaletti, V. De Sabbata, P. Fortint, and C. Gualdi, Nuovo Cim. B **70**, 129 (1970).
  - [14] F. Y. Li, H. Wen, and Z. Y. Fang, Chinese Physics B **22**, 120402 (2013).
  - [15] F. Y. Li, H. Wen, Z. Y. Fang, L. F. Wei, Y. W. Wang, and M. Zhang, Nuclear Physics B

- 911**, 500 (2016).
- [16] F. Y. Li, M. X. Tang, and D. P. Shi, *Phys. Rev. D* **67**, 104008 (2003).
  - [17] F. Y. Li, R. M. L. Baker, Jr., Z. Y. Fang, G. V. Stephenson, and Z. Y. Chen, *Eur. Phys. J. C* **56**, 407 (2008).
  - [18] F. Y. Li, N. Yang, Z. Y. Fang, R. M. L. Baker, G. V. Stephenson, and H. Wen, *Phys. Rev. D* **80**, 064013 (2009).
  - [19] H. Wen, F. Y. Li, and Z. Y. Fang, *Phys. Rev. D* **89**, 104025 (2014).
  - [20] H. Wen, F. Y. Li, Z. Y. Fang, and A. Beckwith, *The European Physical Journal C* **74**, 2998 (2014).
  - [21] D.-P. Shi, F.-Y. Li, and Y. Zhang, *Wuli Xuebao/Acta Physica Sinica* **55**, 5041 (2006).
  - [22] J. Li, F. Y. Li, and Y. H. Zhong, *Chinese Physics B* **18**, 922 (2009).
  - [23] X. Li, S. Wang, and H. Wen, *Chinese Physics C* **40** (2016), 10.1088/1674-1137/40/8/085101.
  - [24] T. Piran, *Rev. Mod. Phys.* **76**, 1143 (2005).
  - [25] B. D. Metzger, T. A. Thompson, and E. Quataert, *Astrophys. J.* **659**, 561 (2007).
  - [26] T. Piran, *Physics Reports* **314**, 575 (1999).
  - [27] W. K. De Logi and A. R. Mickelson, *Phys. Rev. D* **16**, 2915 (1977).
  - [28] K.-H. Rädler, H. Fuchs, U. Geppert, M. Rheinhardt, and T. Zannias, *Phys. Rev. D* **64**, 083008 (2001).
  - [29] C. Thompson, *The Astrophysical Journal* **688**, 1258 (2008).
  - [30] S. R. Kulkarni, S. G. Djorgovski, A. N. Ramaprakash, R. Goodrich, J. S. Bloom, K. L. Adelberger, T. Kundic, L. Lubin, D. A. Frail, F. Frontera, M. Feroci, L. Nicastro, A. J. Barth, M. Davis, A. V. Filippenko, and J. Newman, *Nature* **393**, 35 (1998).
  - [31] S. R. Kulkarni, S. G. Djorgovski, S. C. Odewahn, J. S. Bloom, R. R. Gal, C. D. Koresko, F. A. Harrison, L. M. Lubin, L. Armus, R. Sari, G. D. Illingworth, D. D. Kelson, D. K. Magee, P. G. v. Dokkum, D. A. Frail, J. S. Mulchaey, M. A. Malkan, I. S. McClean, H. I. Teplitz, D. Koerner, D. Kirkpatrick, N. Kobayashi, I. A. Yadigaroglu, J. Halpern, T. Piran, R. W. Goodrich, F. H. Chaffee, M. Feroci, and E. Costa, *Nature* **398**, 389 (1999).
  - [32] D. Eichler, M. Livio, T. Piran, and D. N. Schramm, *Nature* **340**, 126 (1999).
  - [33] R. Narayan, B. Paczynski, and T. Piran, *Astrophysical Journal Letter* **395**, L83 (1992).
  - [34] B. Paczynski, *Acta Astronomica* **41**, 257 (1991).
  - [35] R. D. Blandford and R. L. Znajek, *Monthly Notices of the Royal Astronomical Society* **179**, 433 (1977).

- [36] V. V. Usov, *Nature* **357**, 472 (1992).
- [37] V. V. Usov, *Monthly Notices of the Royal Astronomical Society* **267**, 1035 (1994).
- [38] M. V. Smolsky and V. V. Usov, *Astrophysical Journal* **461**, 858 (1996).
- [39] M. V. Smolsky and V. V. Usov, *The Astrophysical Journal* **531**, 764 (2000).
- [40] G. Drenkhahn and H. C. Spruit, *Astronomy and Astrophysics* **391**, 1141 (2002).
- [41] H. C. Spruit, F. Daigne, and G. Drenkhahn, *Astronomy and Astrophysics* **369**, 694 (2001).
- [42] C. Thompson and R. C. Duncan, *The Astrophysical Journal* **561**, 980 (2001).
- [43] D. Eichler, *Monthly Notices of the Royal Astronomical Society* **335**, 883 (2002).
- [44] B. Zhang and P. Meszaros, *The Astrophysical Journal Letters* **552**, L35 (2001).
- [45] T. A. Thompson, *arXiv:astro-ph/0611368* (2006).
- [46] A. Corsi and P. Mszros, *The Astrophysical Journal* **702**, 1171 (2009).
- [47] Z. G. Dai, *The Astrophysical Journal* **606**, 1000 (2004).
- [48] A. M. Pires, F. Haberl, V. E. Zavlin, C. Motch, S. Zane, and M. M. Hohle, *ASTRONOMY & ASTROPHYSICS* **563**, A50 (2014).
- [49] C. Thompson and R. Gill, *The Astrophysical Journal* **791**, 46 (2014).
- [50] D. Fargion and M. Grossi, *Chinese Journal of Astronomy and Astrophysics* **6**, 342 (2006).
- [51] S. Dall’Osso, G. Stratta, D. Guetta, S. Covino, G. De Cesare, and L. Stella, *A A* **526**, A121 (2011).
- [52] C. Thompson and R. C. Duncan, *Monthly Notices of the Royal Astronomical Society* **275**, 255 (1995).
- [53] C. Thompson and R. C. Duncan, *The Astrophysical Journal* **561**, 980 (2001).
- [54] Y. Kaneko, E. Gogus, C. Kouveliotou, J. Granot, E. Ramirez-Ruiz, A. J. van der Horst, A. L. Watts, M. H. Finger, N. Gehrels, A. Pe’er, M. van der Klis, A. von Kienlin, S. Wachter, C. A. Wilson-Hodge, and P. M. Woods, *The Astrophysical Journal* **710**, 1335 (2010).
- [55] B. D. Metzger, T. A. Thompson, and E. Quataert, *AIP Conference Proceedings* **1000**, 413 (2008).
- [56] A. I. Ibrahim, T. E. Strohmayer, P. M. Woods, C. Kouveliotou, C. Thompson, R. C. Duncan, S. Dieters, J. H. Swank, J. van Paradijs, and M. Finger, *The Astrophysical Journal* **558**, 237 (2001).
- [57] J. J. Jia, Y. F. Huang, and K. S. Cheng, *The Astrophysical Journal* **677**, 488 (2008).
- [58] G. L. Israel, P. Romano, V. Mangano, S. Dall’Osso, G. Chincarini, L. Stella, S. Campana, T. Belloni, G. Tagliaferri, A. J. Blustin, T. Sakamoto, K. Hurley, S. Zane, A. Moretti,

- D. Palmer, C. Guidorzi, D. N. Burrows, N. Gehrels, and H. A. Krimm, *The Astrophysical Journal* **685**, 1114 (2008).
- [59] J. Goodman, *Astrophysical Journal* **308**, L47 (1986).
- [60] B. Paczynski, *Astrophysical Journal* **308**, L43 (1986).
- [61] T. Piran, A. Shemi, and R. Narayan, *Monthly Notices of the Royal Astronomical Society* **263**, 861 (1993).
- [62] B. C. Thomas, C. H. Jackman, A. L. Melott, C. M. Laird, R. S. Stolarski, N. Gehrels, J. K. Cannizzo, and D. P. Hogan, *The Astrophysical Journal Letters* **622**, L153 (2005).